

# Design Requirements and Component Down Selection Process for an Aperture Masking Instrument at the Magdalena Ridge Observatory 2.4m Telescope

Luke M. Schmidt<sup>1</sup>, S. W. Teare<sup>1</sup>, D.J. Westpfahl<sup>1</sup>, C.A. Jurgenson<sup>2</sup>  
<sup>1</sup>New Mexico Institute of Mining and Technology <sup>2</sup>Magdalena Ridge Observatory, New Mexico Institute of Mining and Technology



## Introduction

The design of a new instrument requires careful consideration of all components to ensure that design specifications are met while staying within the prescribed budget. This poster presents the down selection process for the major components of a new instrument for the Magdalena Ridge Observatory 2.4m telescope. This instrument is designed primarily for aperture masking at optical wavelengths, a technique that converts a single aperture into a multi-aperture Michelson stellar interferometer. With minor modification this instrument can also be used for millimag photometry, millisecond photometry and other high speed imaging techniques. Three main components are described: An optical support structure and telescope interface designed to minimize flexure, vibration and optical alignment changes, the optical system necessary to re-image the primary aperture and produce fringes at scales necessary for Nyquist sampling of interference fringes, and the CCD performance required for high-frame-rate, low-noise images.

## References

- Baldwin, J.E. et al. 1986Natur.320. 595B
- Loos, G.C. Appl. Opt., Vol. 32, No. 1, p. 52 - 56
- Buil, C. "CCD Astronomy", Willmann-Bell, 1991
- http://www.pricetoneinstruments.com/library/references.aspx, accessed 28May2009

## Acknowledgements

- LANL-NMT-MOU UCDDR Funding
- New Mexico Space Grant Consortium
- NMT Office of the Vice President for Research and Development
- NMT Graduate Student Association Travel Grant

## Structure

Several different construction materials were considered for the support structure. The instrument will be mounted on one of the Nasmyth foci on the MRO 2.4m telescope. The raw data coming out of this instrument is in the form of interference fringes. Fringe stability is dependent on maintaining optical alignment throughout the system. The support structure must be capable of supporting the optics and cameras without flexure as well as being an athermalized design. Three designs were considered utilizing varying amounts of commercially available components.

The first design, (figure 1) was a completely commercially available design utilizing a threaded tube component mounting system. This system consists of tubular lens and mirror holders that are connected together via threaded aluminum tubes. Optical distances are controlled via spacers and varying tube lengths. This design was discarded due to limitations in optics sizes (no larger than 40mm in diameter). This design would have also required an additional support structure to prevent flexure as minimizing the number of optical surfaces led to a "straight through" design that would have extended from the side of the telescope several meters.

The second design, (figure 2) was a carbon fiber laminate and truss system. Carbon fiber was selected as an option due to its superior thermal stability (a properly constructed composite can have essentially zero CTE), as well as its stiffness. The design consisted of a carbon fiber laminated panel on which the optics were mounted, supported by a box shaped truss system. While very light, this design was discarded due to its lack of configuration flexibility. In order to mount the optics to the laminated panel, metal inserts must be accurately located and epoxied into the panel. If the spacing of a component changes, or the instrument needs modification in the future, new holes must be drilled for inserts. This requires complete instrument disassembly.

The design that was chosen, (figure 3) consists of a commercially available optical breadboard supported and attached to the Nasmyth focus by a custom tubular support. The support structure attaches to the Nasmyth focus via an aluminum mounting plate. This plate is connected to a tubular frame that supports the optical breadboard. The internal structure of the optical table incorporates a honeycomb structure to resist flexure and an internal damping system to minimize vibrations. The surface has standard threaded holes to allow for flexibility in placing optics and a cost under \$2000.00. The tubular structure that holds the optical breadboard is very simple in design, essentially a shelf, reinforced to resist vertical flexure due to gravity. The Nasmyth port mounting simplifies the design as well, as the optical breadboard is always level. The available Nasmyth port does not have an instrument rotator.

Other smaller components, such as filter wheels, optics mounts and a light enclosure were chosen on a basis of cost and time investment. Filter/Mask wheels will come from Finger Lakes Instruments due to their flexibility in filter size, relatively low cost and easy software integration. External light control will be accomplished by lightweight panels that will attach to the support structure, controlling dust and allowing easy access. Optics mounts will be from commercially available sources due to their compatibility with the optical breadboard and easy availability. Some custom mounts may need to be constructed to support the camera and filter wheels, but these should be very simple in design and relatively inexpensive.

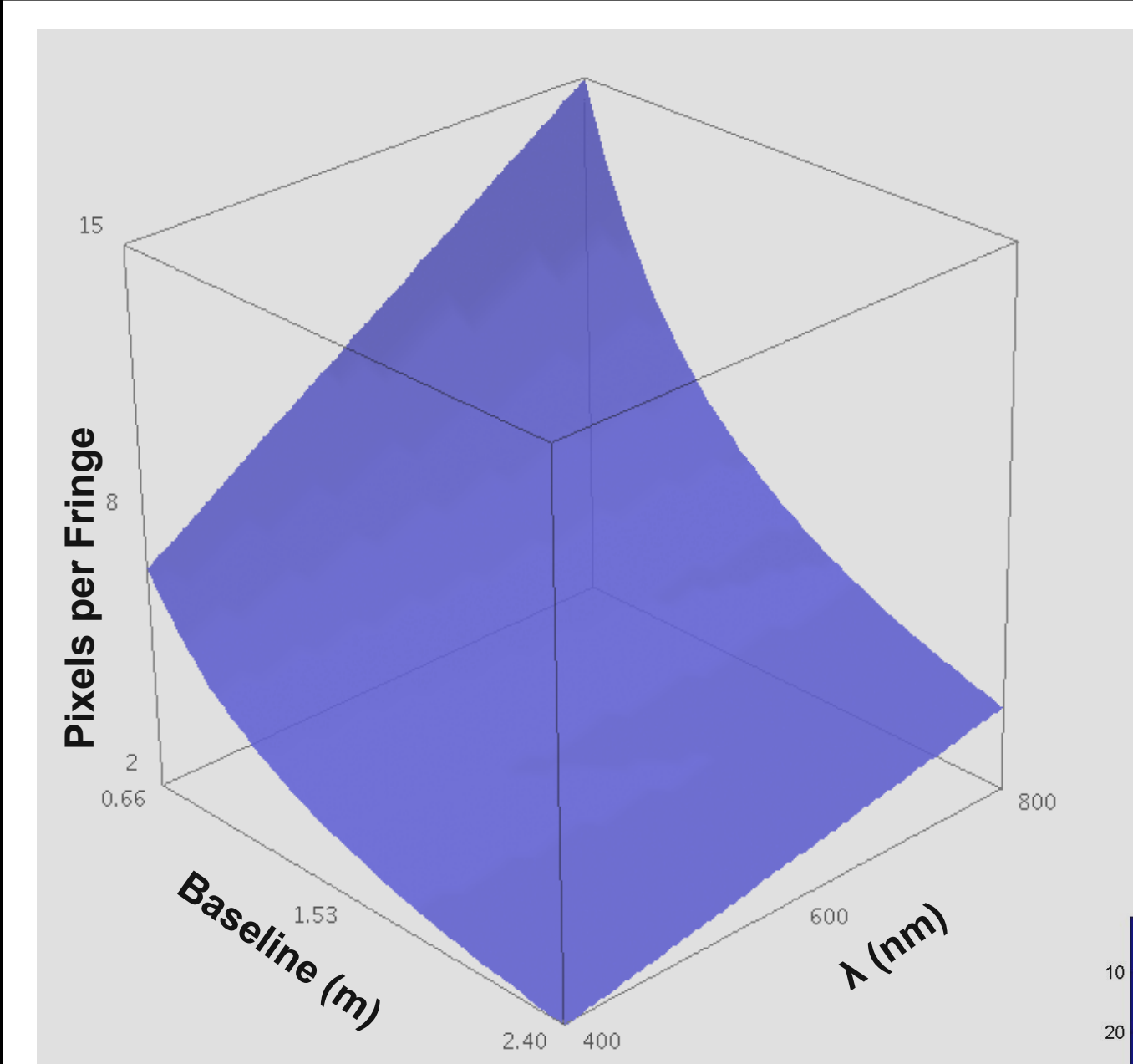
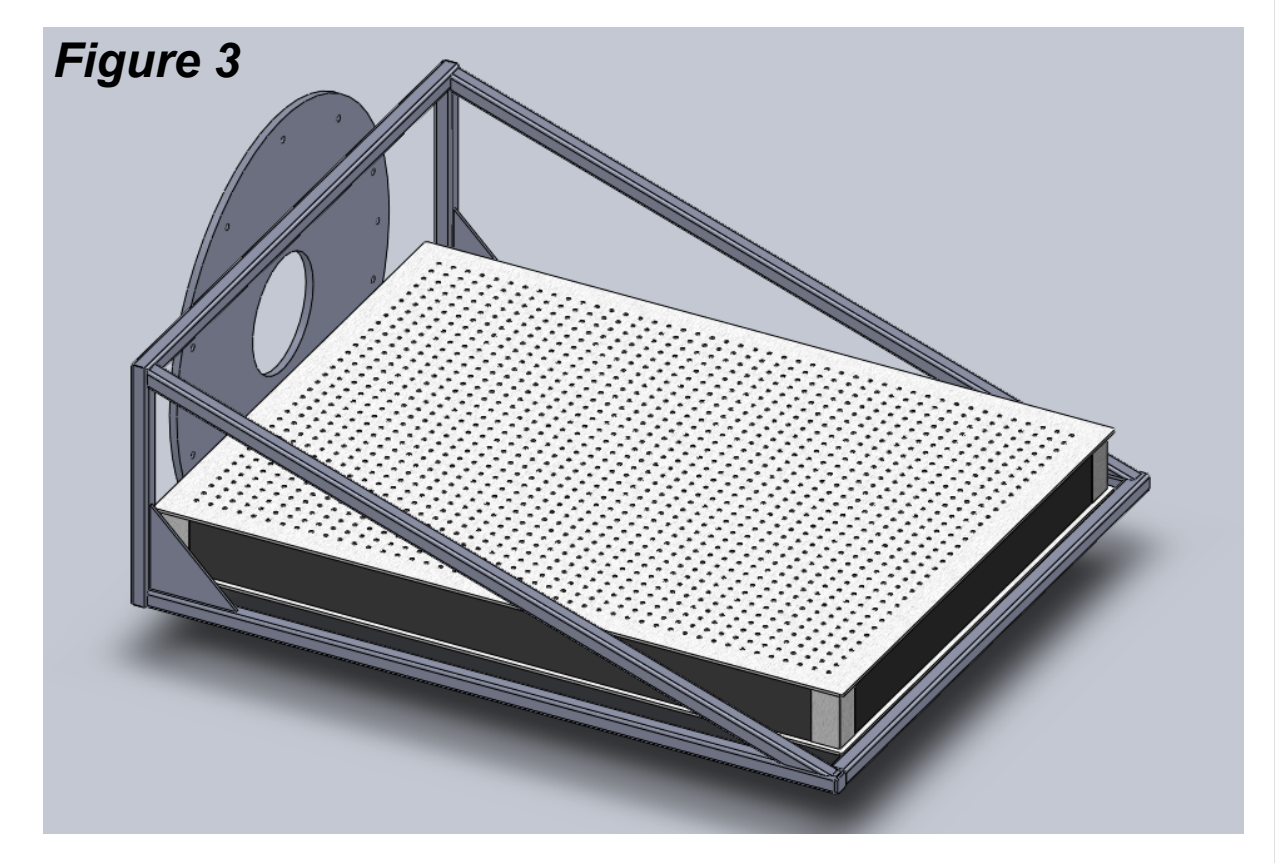
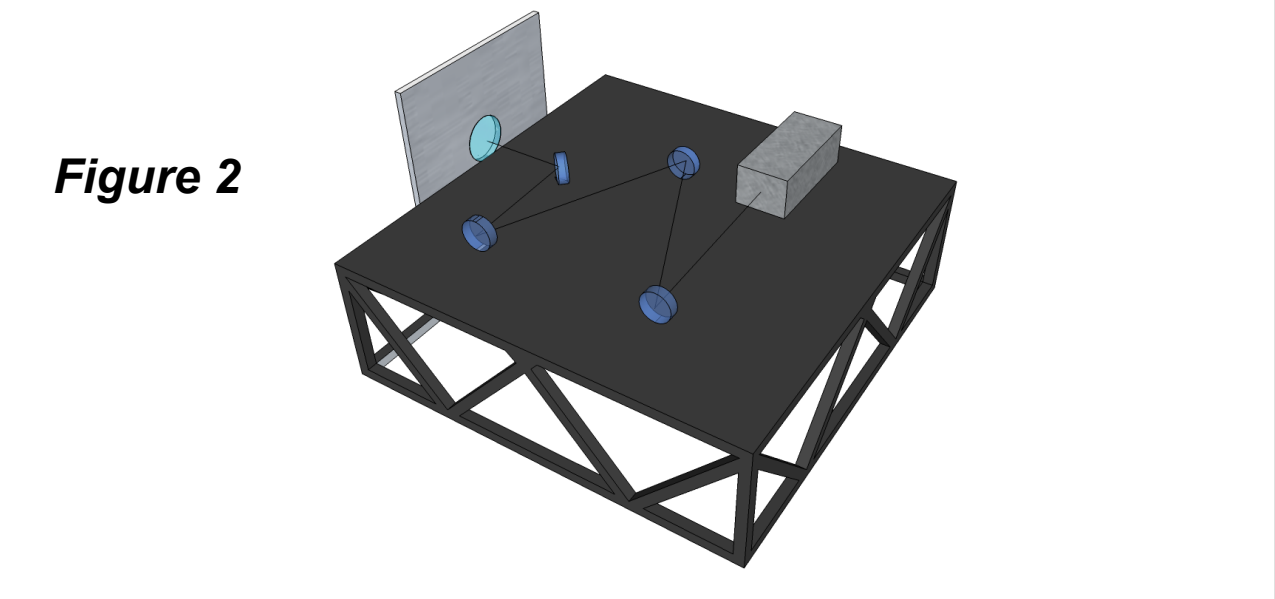
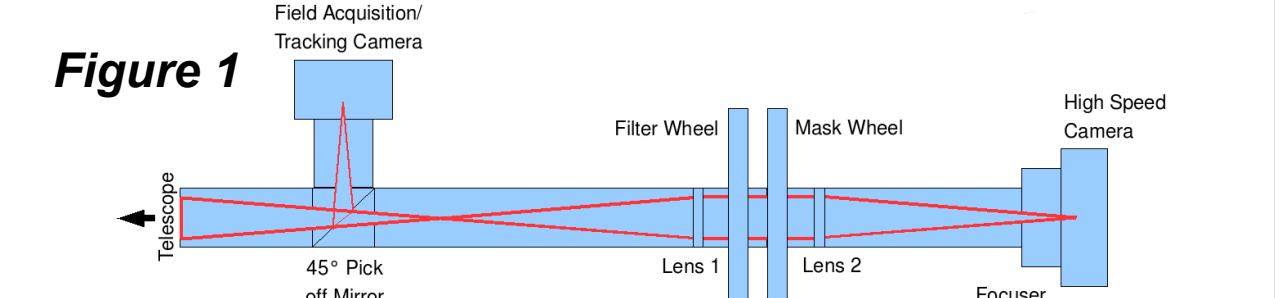
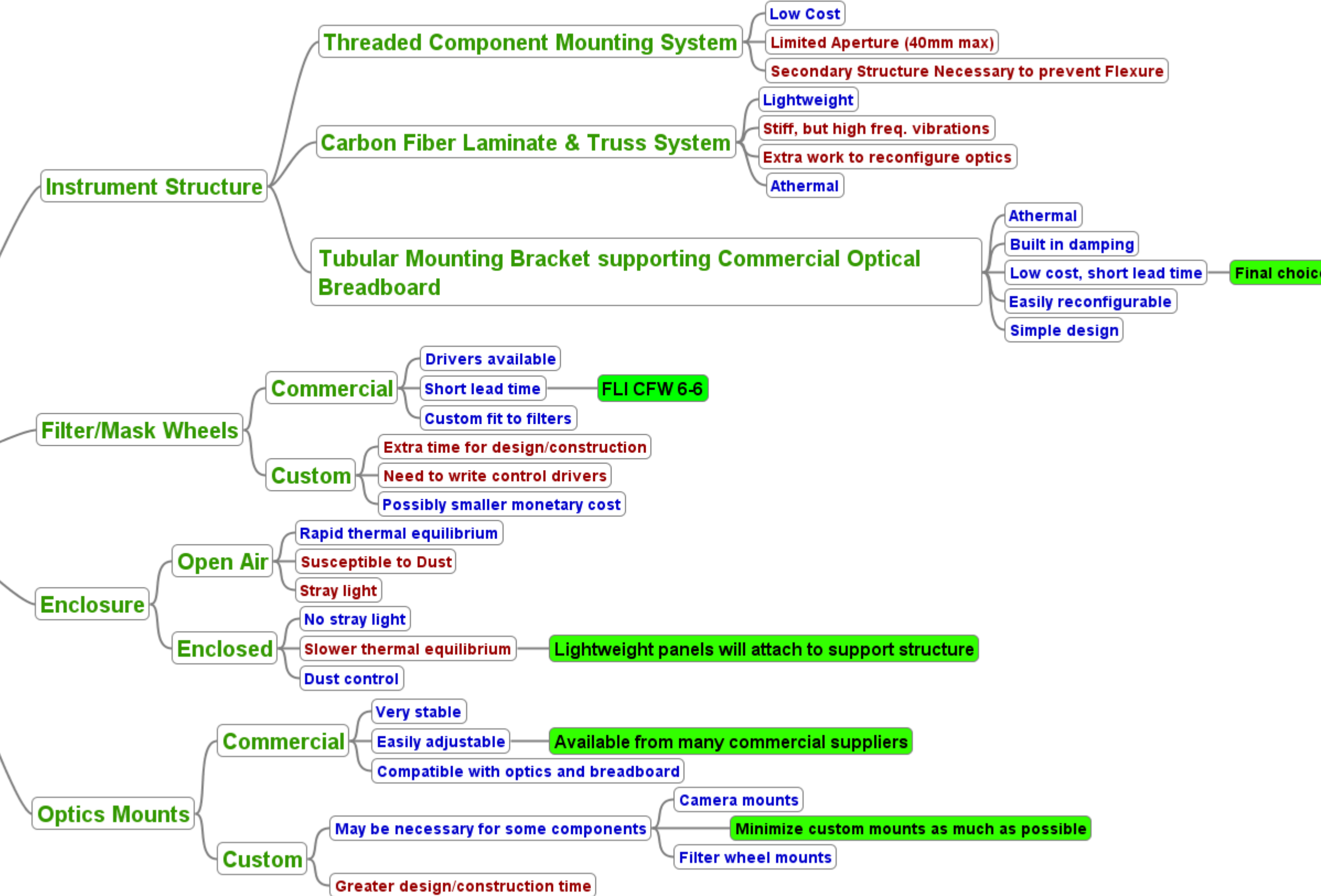


Figure 4 Fringe Sampling as a function of baseline and wavelength. The design specifications require that at the longest baseline and shortest wavelength the fringes are still Nyquist sampled as shown by the lowest point on the plot. Essentially this requirement sets the focal length of the instrument. This plot is based on 16µm pixels and requires an effective focal length of 192m (f/80).

Figure 5 Sample fringe pattern produced by a three hole mask. Overall spot size is set by the individual sub apertures. Courtesy of Scott Teare.

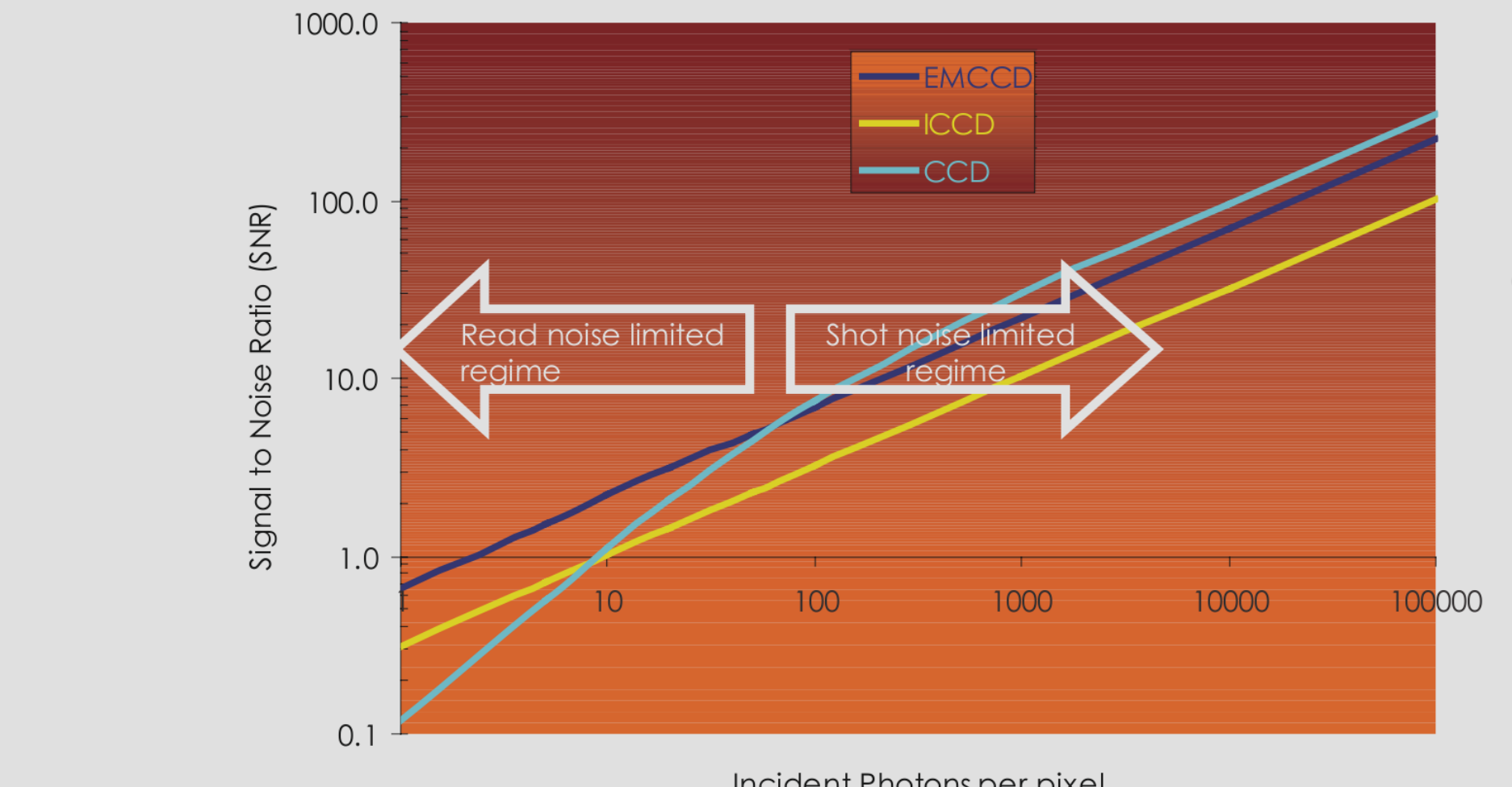
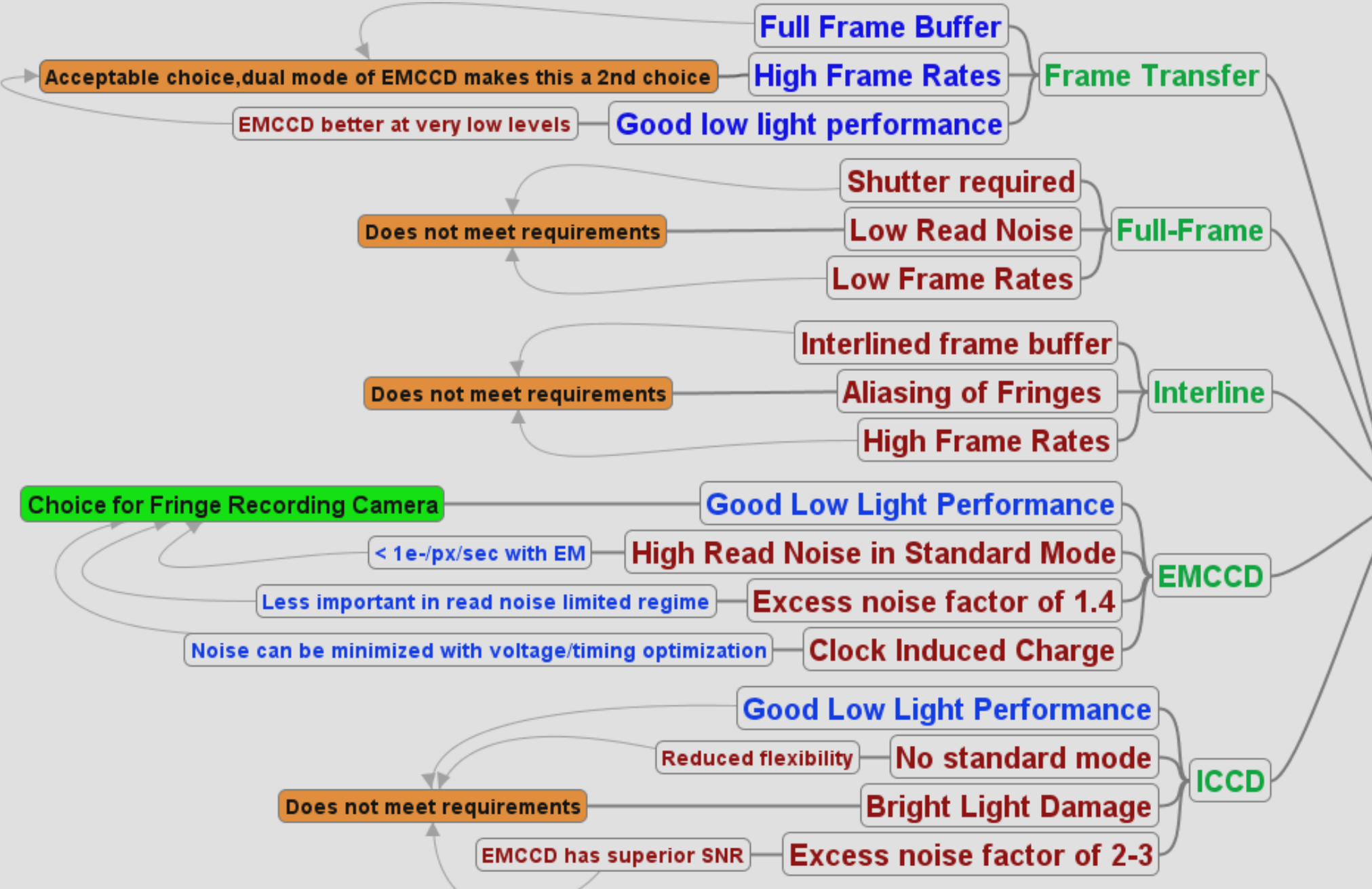


Figure 6 This plot shows the advantages of different CCD architectures at different signal levels. For long exposure images, traditional CCDs have a higher SNR due to the lack of the excess noise factor from the statistical nature of the electron multiplication process. At low signal levels, EMCCDs have a clear advantage, especially at high frame rates where read noise is high. Image courtesy of Princeton Instruments. Copyright 2009. All rights reserved.



## CCD

There are two cameras that are a part of AMASING. The first is a guide camera. It is located after a pick off mirror that directs the majority of incident light to the re-imaging optics. No focal length modification is applied, the light is filtered and then imaged by the camera. Design requirements are that the field of view be large enough to acquire a guide star and image acquisition time is short enough for the guiding interval. The Alta U6 from Apogee instruments was chosen for this camera. The field of view is 4'x4' and 0.23"/px.

The primary camera has much more stringent design requirements. This camera is the fringe recording camera, it records the interference pattern formed by the aperture mask as shown in figure 5. The integration time must be on the same order as the coherence time of the atmosphere at the wavelength selected by the narrow band filter. This requires the ability to take exposures on the order of milliseconds at frame rates of at least 30fps. The specifications of the CCD determine the requirements of the optical layout that produces the fringes. The pixel size determines the sampling of the fringes at a given focal ratio. The larger the pixels the higher the magnification necessary to Nyquist sample fringes on the longest baselines. Blue light aperture masking will have the smallest fringe spacing, so that was selected as the minimum design requirement. Figure 4 shows the fringe sampling of the instrument designed to work at baselines of 0.66-2.4m and λ=400-800nm.

Of the five chip architectures listed in the selection tree to the left, three were almost immediately discarded as possibilities. Full frame chips have very low frame rates and require a shutter to prevent smearing. Because we are sampling fringes the interline architecture was not chosen, despite its high frame rates, due to the possibility of aliasing of the fringes. Finally, the ICCD, while having excellent low light capabilities, lacks flexibility in that it does not have a non intensifying read mode, can be damaged by bright light and has a high excess noise factor. This left the traditional frame transfer CCD and the Electron Multiplying CCD, also a frame transfer architecture.

The choice between these two detector types is dependent on if the incident fringes are in the shot noise limited or read noise limited regime as shown in figure 6. To determine the correct choice, a radiative transfer model was constructed, following the work of Loos<sup>2</sup> and Buil<sup>3</sup>. This model predicts that incident photon levels will be in the read noise limited regime, where the EMCCD shows a clear advantage. The ability to run in non amplifying mode gives the EMCCD additional flexibility for use in higher light situations and has relatively low read noise for long integrations with slower read rates. The chosen CCD chip is the e2v CCD97, we are currently comparing available cameras that utilize this chip.

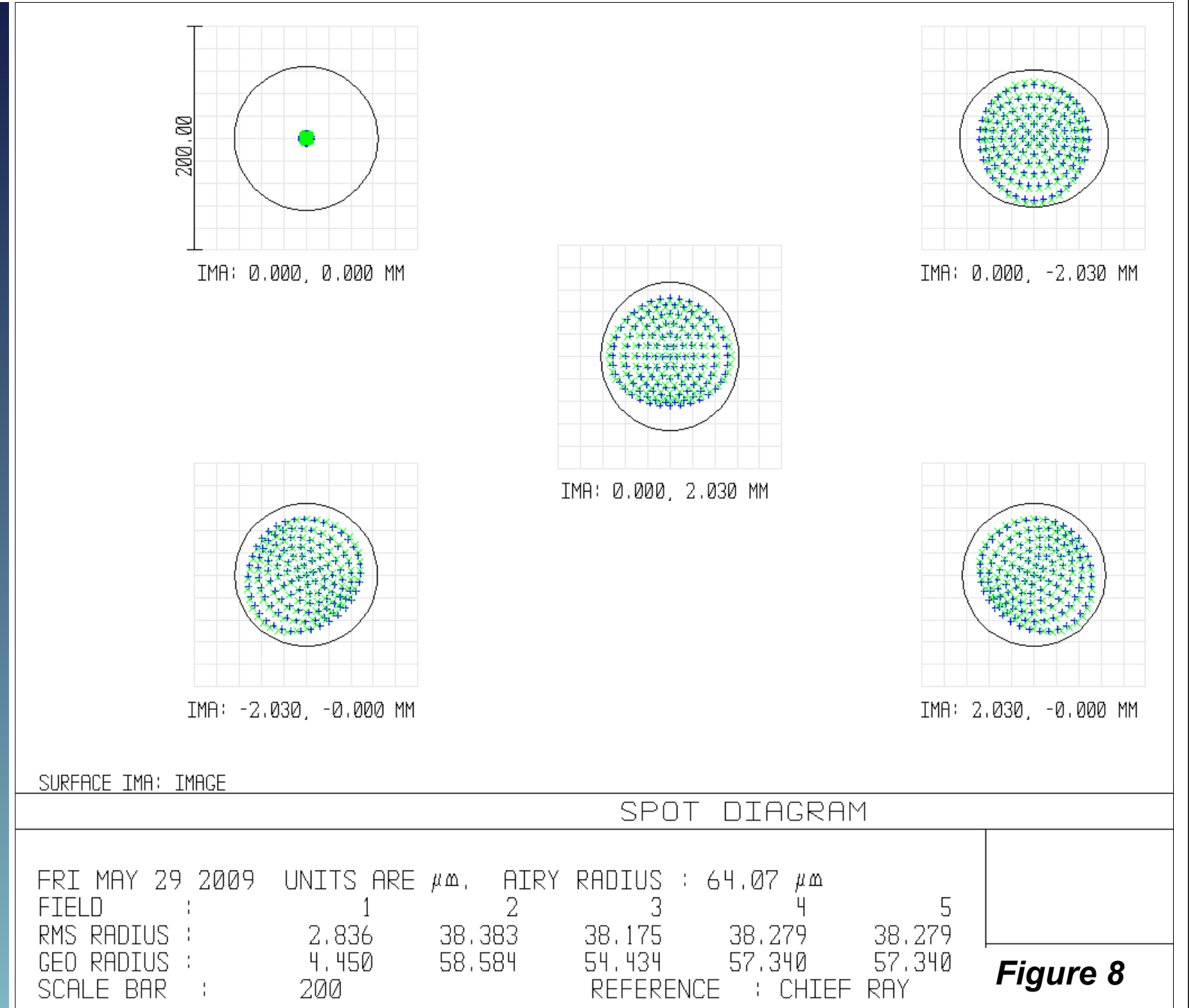
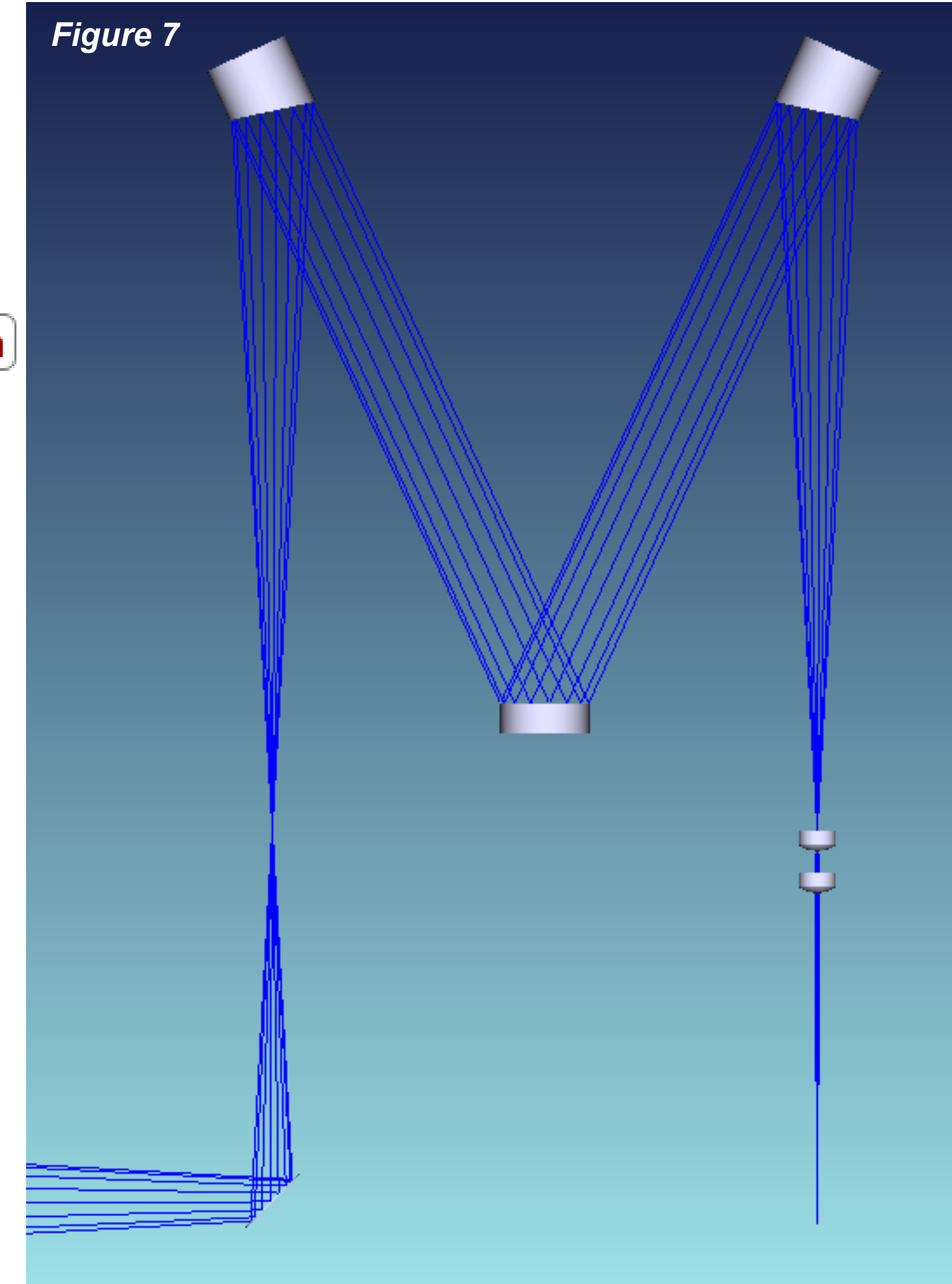
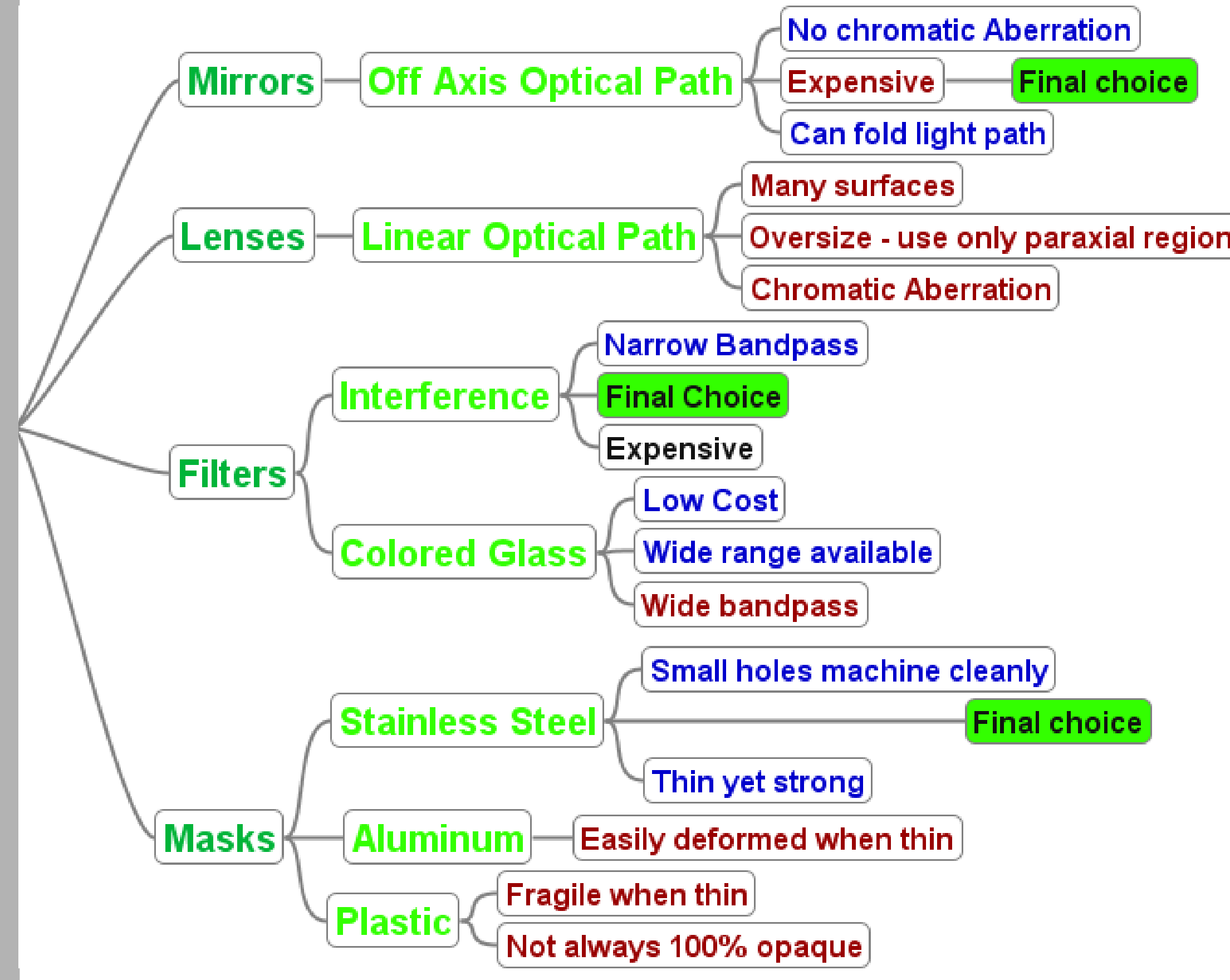
## Optics

Two types of optics were considered for this instrument, refractive and reflective. The first iteration of the design used all commercially available achromatic refractive elements due to their low cost and the ability to construct the entire aperture masking optical train on a single optical axis. This design had a minimum of optical elements to maximize light throughput. However, refractive elements suffer from chromatic aberrations and in order to minimize other aberrations, only the paraxial region of the lens can be used. This requires oversizing the optics. The current design uses reflective optics, chosen for their lack of chromatic aberration, ability to develop a compact folded design and with enhanced coatings offer low transmission losses.

Light from the telescope first encounters a dichroic filter. This filter will transmit part of the spectrum and reflect part of the spectrum. It is chosen so that the transmitted part goes to the guide camera and, with greater than 98% reflectivity, the wavelengths desired for aperture masking are directed to the re-imaging optics. This allows for guiding with minimal light lost for aperture masking.

A folded off axis design was chosen for the re-imaging optics. By using off axis parabolas there are no obstructions in the resulting collimated beam. After reflection off of the dichroic, the first off axis parabola re-images the primary aperture, its focal ratio is matched to that of the telescope. Once collimated, the light passes through a narrow band interference filter and then through the mask. Filters will be narrow band interference filters to minimize fringe visibility loss due to higher order fringe spread for a wide spectral bandwidth. The mask is constructed out of thin stainless steel and sized to fit in standard filter wheels to allow for easy mask selection. The sub-apertures in the masks will be made via Electrical Discharge Machining (EDM) to produce holes with very clean edges, minimizing diffraction effects. A fold mirror is placed before the second OAP to make the design more compact and can be replaced with a diffraction grating to convert the instrument into a spectrometer.

The final part of the optical path is needed to achieve the necessary image scale for sampling interference fringes at the longest baselines. From the camera selection process it was found that the optimal focal ratio is f/80. The telescope is f/8.8 for a magnification of 9x. Using a Lister microscope objective design with two 25mm diameter achromatic lenses, each with focal length of 30mm gives the necessary magnification. See figure 7 for the optical layout and figure 8 for the spot diagram of the complete system.



Spot diagram for the complete optical system without aperture masks at 656.3nm. The field is equivalent to the central 256x256 pixels on the CCD (16µm pixels).